

Coupling Basin- and Site-Scale Inverse Models of the Española Aquifer

by Elizabeth H. Keating¹, Velimir V. Vesselinov¹, Edward Kwicklis¹, and Zhiming Lu¹

Abstract/

Large-scale models are frequently used to estimate fluxes to small-scale models. The uncertainty associated with these flux estimates, however, is rarely addressed. We present a case study from the Española Basin, northern New Mexico, where we use a basin-scale model coupled with a high-resolution, nested site-scale model. Both models are three-dimensional and are analyzed by codes FEHM and PEST. Using constrained nonlinear optimization, we examine the effect of parameter uncertainty in the basin-scale model on the nonlinear confidence limits of predicted fluxes to the site-scale model. We find that some of the fluxes are very well constrained, while for others there is fairly large uncertainty. Site-scale transport simulation results, however, are relatively insensitive to the estimated uncertainty in the fluxes. We also compare parameter estimates obtained by the basin- and site-scale inverse models. Differences in the model grid resolution (scale of parameter estimation) result in differing delineation of hydrostratigraphic units, so the two models produce different estimates for some units. The effect is similar to the observed scale effect in medium properties owing to differences in tested volume. More important, estimation uncertainty of model parameters is quite different at the two scales. Overall, the basin inverse model resulted in significantly lower estimates of uncertainty, because of the larger calibration dataset available. This suggests that the basin-scale model contributes not only important boundary condition information but also improved parameter identification for some units. Our results demonstrate that caution is warranted when applying parameter estimates inferred from a large-scale model to small-scale simulations, and vice versa.

Introduction

The most straightforward method to obtain fine grid resolution in the region of interest and maintain consistency with a larger-scale flow field is to refine the large-scale model grid selectively (Kernodle and Thorn 1995; Tiedeman et al. 1998; Meier 1999; Keating et al. 2000a; Vesselinov and Neuman, 2001). This method, however, may not produce sufficient resolution in the area of interest without significantly increasing the total number of grid elements; this is a particularly severe problem with finite-difference methods. A more complex approach is to build nested models (telescopic mesh refinement) (Ward et al. 1987; Keating and Bahr 1998; Leake et al. 1998; Walker and Gylling 1998; Hunt et al. 2001; Zyvoloski et al. 2002). Nested models can be coupled either through specified-flux or specified-head boundary conditions; specified-flux conditions

have the advantage of conserving mass in the coupled model system. This is especially important if the site-scale model is used to predict the effect of pumping (Giudici et al. 2001). For transient simulations, it may be necessary to specify transient flux boundary conditions (Anderson and Woessner 1992).

In this paper, we discuss parameter uncertainty in site-scale and basin-scale models and investigate two aspects of coupling nested models. The first is the potential differences between estimates of parameters and parameter uncertainty provided by inverse modeling at the two scales. Adjusting parameters within the site-scale model independently of basin-scale calibration is common (Hunt et al. 2001; Zyvoloski et al. 2002). Calibration of the two models simultaneously, even with weak coupling, has not been reported in the literature. The second aspect is related to evaluation of sources of uncertainty in the site-scale model. There will be a number of possible sources of uncertainty for any prediction made using the site-scale model. We have explored, for example, the influence of parameter uncertainty on ground water flow directions (Keating et al. 2000b). In this paper, we apply a method for quantifying

¹Earth and Environmental Sciences Division, Los Alamos National Laboratory, Los Alamos, NM 87545; ekeating@lanl.gov, vv@lanl.gov, kwicklis@lanl.gov, zhiming@lanl.gov

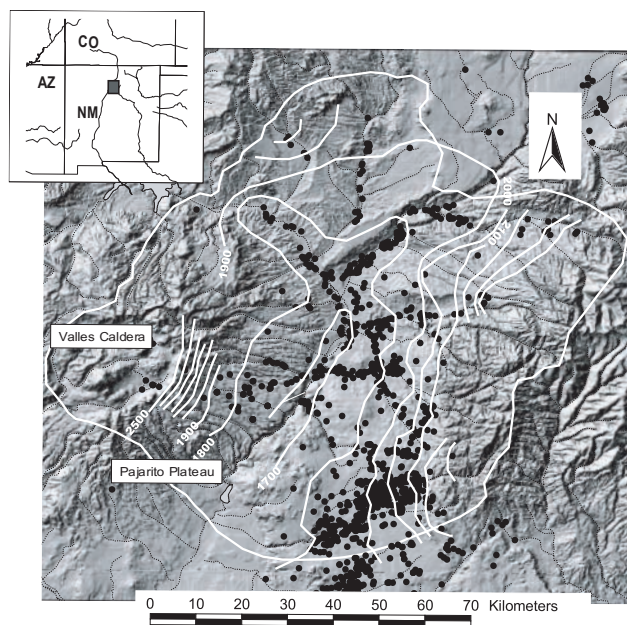


Figure 1. Topographic map of Española Basin; white contours represent water levels (100 m interval) and black dots indicate location of wells used to develop contours. Inset shows the location of the basin in northern New Mexico.

uncertainty in boundary fluxes and determining the sensitivity of travel time predictions to this uncertainty.

The aquifer within the Española Basin is a major source of water for pueblos, municipalities, and numerous agricultural communities in northern New Mexico. Los Alamos National Laboratory (LANL) is situated on the Pajarito Plateau, which lies along the western margin of the basin (Figure 1). Because of concern over potential impact of present and past laboratory activities on the ground water resource, LANL is conducting an extensive ground water characterization program (LANL 1998). Flow and transport modeling has been a vital element to this program and has been used to test and improve the conceptual model of the aquifer, to site new characterization wells, and to predict the fate and transport of contaminants detected during drilling.

To support the goals of the characterization program, we require models with sufficiently high resolution to capture complex hydrostratigraphy known to be present beneath the site. Several numerical ground water flow models have been developed for the region (Hearne 1985; McAda and Wasiolek 1988; Frenzel 1995), primarily to address water resource issues, and do not have sufficient grid resolution for our purposes. Owing to computational limitations, our requirements for high grid resolution at the site scale prevent us from extending the spatial extent of our model to natural hydrologic boundaries (in our case, the margins of the Española Basin). Unfortunately, existing regional models do not have sufficient lateral extent west of LANL to be used to specify meaningful boundary conditions for a site-scale model. We have therefore developed new three-dimensional, control-volume, finite-element models (Keating et al. 1999; Keating et al. 2000a), building on previous work by others in the region (Purtymun 1984; Hearne 1985; McAda and Wasiolek 1988; Daniel B.

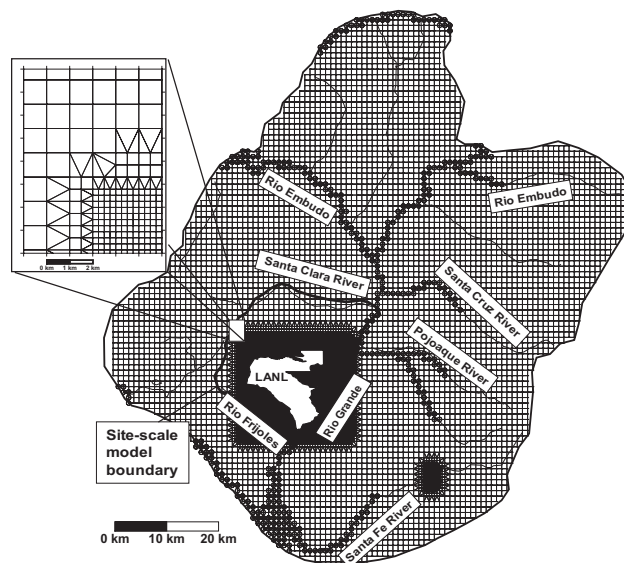


Figure 2. Basin model grid (plan view) with site-model boundaries indicated. Inset shows northwest corner of octree mesh refinement region. Circles show locations of specified head nodes along rivers and basin margins. Asterisk along eastern boundary indicates latitude of cross sections in Figure 3.

Table 1
Comparison of Model Attributes, Calibration Data,
and Goodness-of-Fit Statistics

	Basin-Scale	Site-Scale
Grid resolution:		
Number of nodes	277,951 (91,872 within site-scale model region)	172,741
Number of tetrahedral elements	1,528,407	949,835
Number of calibration targets:		
Pre-development flux estimates	7	0
Pre-development head measurements	81	26
Transient head measurements	76	66
Total	164	92
Number of estimated parameters (the initial number in parentheses):		
Recharge parameters	2 (3)	1 (3)
Hydrostratigraphic-unit permeabilities	18 (35)	10 (26)
Specific storage	1 (1)	1 (1)
Total	21 (38)	12 (30)
Degrees of freedom:	143	80
Objective function (sum of squared weighted residuals):	2.37×10^5 (1.40×10^5 for the targets common for both models)	1.33×10^5
Log Likelihood function:	-562	-916

Stephens & Associates 1994). Initially we were able to obtain a relatively high-resolution grid for the site and extend lateral boundaries to basin boundaries using octree mesh refinement (OMR). The octree refinement is performed (Trease et al. 1996) by subdividing selected octahedral cells in the original orthogonal and structured grid into

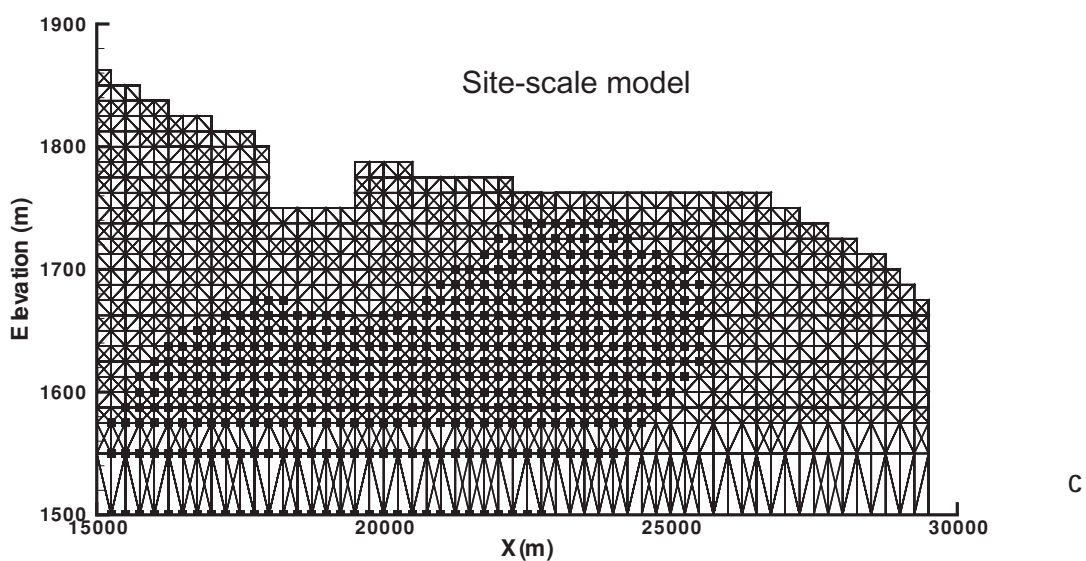
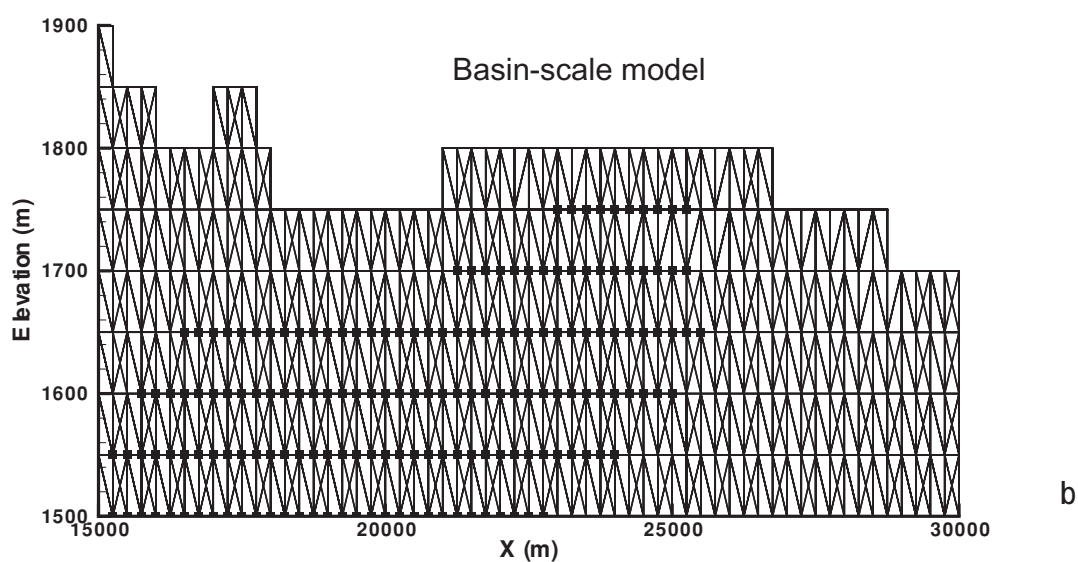
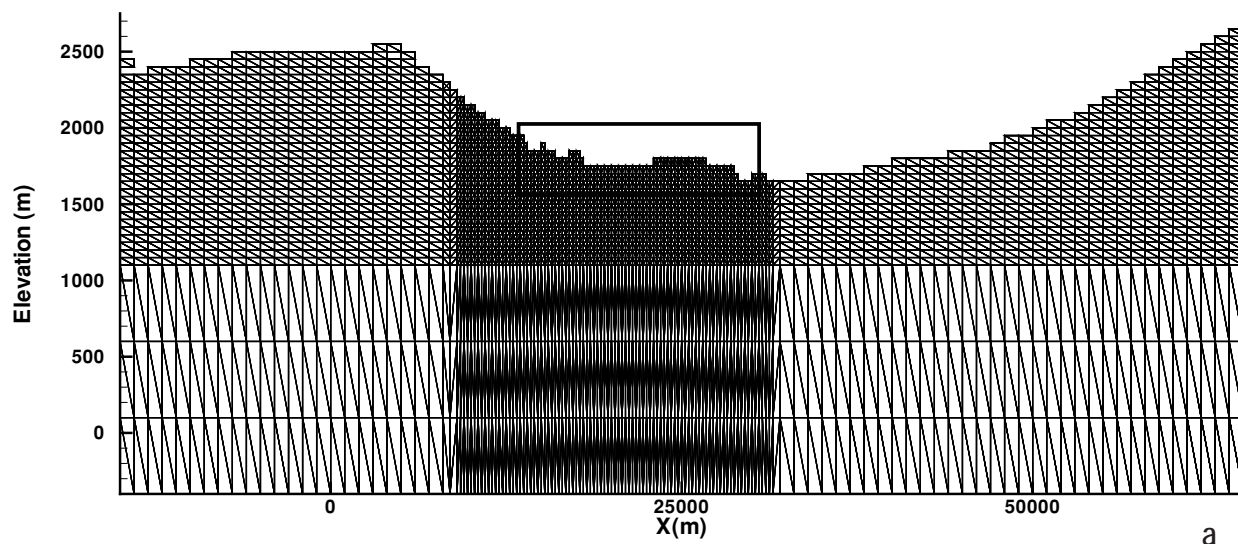


Figure 3. Cross-sectional views of basin- and site-scale grids: (a) basin grid; box shows location of views in (b) and (c); (b) zoomed basin grid; (c) zoomed site grid. Black circles in (b) and (c) show nodes identified as basalt.

eight octahedral cells. The refined model provided very good control on mass flux through the system and reasonably detailed site-scale transport calculations; however, it ultimately failed to provide sufficient vertical resolution at the site scale to capture significant hydrostratigraphic features with adequate resolution. To achieve the higher resolution, we are coupling two models: this OMR basin-scale model with relatively coarse vertical resolution (50 m) to a site-scale model with an increased vertical resolution (12.5 m). Our modeling approach uses the FEHM (finite element heat and mass transfer) code (Zyvoloski et al. 1997) to simulate flow and transport and the PEST code (Doherty, 2000) to estimate parameters and evaluate uncertainty of model parameters and predictions (Keating et al. 2000a; Keating and Vesselinov 2001; Vesselinov et al. 2001).

Hydrologic Setting

The Española Basin (Figure 1) is in northern New Mexico. It is one of a series of basins located within the Rio Grande Rift zone, a tectonic feature that extends from northern Colorado to the south into Mexico. Elevations within the basin range from more than 3800 m along peaks in the surrounding mountain ranges to ~1700 m at the Rio Grande near the basin outlet. Vegetation is predominately ponderosa pine forest at higher elevations and piñon pine/juniper at lower elevations (Spiegel and Baldwin 1963, p. 17).

The aquifer comprises predominately Santa Fe Group rocks, which are poorly consolidated basin-fill sediments reaching more than 3000 m in thickness near the basin axis (Cordell 1979). Ground water also occurs in older crystalline rocks along the eastern and northern basin margin and in younger volcanic lavas and volcanoclastic sedimentary rocks in the vicinity of the Pajarito Plateau to the west (Purtymun and Johansen 1974; Coon and Kelly 1984; Daniel B. Stephens & Associates 1994).

The vadose zone is ~0 to 60 m thick in most parts of the basin, much thicker on the Pajarito Plateau (up to 350 m) where perched aquifers also exist. Contours of water level data (Purtymun et al. 1995; U.S. Geological Survey 1997) indicate that hydraulic gradients are generally toward the Rio Grande (Figure 1). Water enters the aquifer as interflow from basins to the north and as recharge. Water leaves the aquifer at numerous water supply and irrigation wells, as interflow to basins to the south, and to the Rio Chama, the Rio Grande and the lower reaches of its tributaries. Median monthly flow, calculated using USGS average monthly flow data for the last 80 years, is 26.0 m³/sec along the Rio Grande (at Otowi Bridge) and 10.0 m³/sec along the Rio Chama (at Chamita) (USGS 2000). Because of recent exploitation of ground water resources in the basin, some reaches of these rivers and their tributaries, which were once ground water discharge zones, may now be recharging the aquifer.

The climate is semiarid; annual total precipitation ranges from 18 to 86 cm/year. Precipitation increases with elevation (Spiegel and Baldwin 1963). Recharge is thought to occur primarily in the higher elevations—estimates based on water budget and chloride mass-balance methods

range from 7% to 26% of total precipitation (Anderholm 1994; Wasiolek 1995). Little or no recharge occurs at lower elevations other than along stream channels because of low precipitation rates and high evapotranspiration demand (Anderholm 1994).

Model Development

Three-dimensional ground water models have been developed using FEHM (Zyvoloski et al. 1997); computational grids were generated using LaGriT (Trease et al. 1996). The computational grid for both the basin- and site-scale models are shown in Figures 2 and 3; grid characteristics are summarized in Table 1. The structure of the two models are identical, except for the increased vertical resolution of the site-scale model and the smaller lateral extent.

The northern and southern boundaries of the basin model were located according to structural transitions between the Española Basin and neighboring basins where basin-fill sedimentary rocks are relatively thin. The eastern boundary corresponds to a topographic divide; the western boundary is a combination of topographic divides and the western margin of the Valles Caldera. These lateral boundaries are assumed to be primarily no-flow, although in limited areas inter-basin flow is allowed to occur through specified head nodes (Figure 2). Along the northern boundary, we allow flow to occur through specified head nodes representing ground water in the alluvium beneath the Rio Chama and Rio Grande and along the basin margin to the far north. Along the southern boundary, we also allow flow through specified head nodes placed in a broad area beneath and adjacent to the Rio Grande. There is no data with which to compare the model predictions of these inter-basin fluxes. We do, however, expect them to be small compared to the total mass flux through the basin as suggested by flux estimates reported by McAda (1988), Kernodle and Thorn (1995), and data presented by Coon and Kelly (1984). There is also outflow to the west of Valles Caldera along the Jemez Canyon; we use streamflow data from the Jemez River to estimate this flux.

The lateral boundaries for the site-scale model (Figure 2) were chosen to coincide with the Rio Grande (to the west), the Santa Clara River (to the north), the Rio Frijoles (to the south), and the topographic divide defining the eastern rim of the Valles Caldera (to the west). Minor discrepancies do exist between actual model boundary locations and these geographic and hydrologic features. Our initial hypothesis is that little or no flow crosses these boundaries; testing this hypothesis is one objective of coupling the site- and basin-scale models.

The upper surface of the model coincides with the top of the saturated zone. Along this surface, nodes are either no-flow, specified-flux (precipitation recharge), or specified-head (major rivers). Major rivers include the Rio Chama, Rio Grande, and the lower reaches of the Santa Fe, Santa Cruz, Embudo, and Pojoaque rivers. Lacking data on riverbed hydraulic conductivity throughout the basin, we assume that there is no contrast in the permeability between riverbeds and aquifer sediments. This assumption is undoubtedly a simplification of actual hydrologic proper-

ties. By evaluating the model calibration and simulated river/aquifer fluxes (described later) we will test the impact of this simplifying assumption.

In our study, it is important to estimate not only the total amount but also the spatial distribution of ground water recharge from precipitation within the basin with corresponding estimates of uncertainty. However, this requires that our recharge model can be parameterized and the respective parameters can be included in the inverse process. Although actual spatial and temporal patterns of recharge in the basin are undoubtedly complex, we use a very simple model that takes advantage of the strong elevation dependence of precipitation in the basin. We also assume recharge is constant in time. We define ground water recharge (R) over the model domain as follows:

$$R(x,y) = \alpha \xi(x,y) \cdot P [Z(x,y)] \quad (1)$$

$$\xi(x,y) = \begin{cases} 1 & Z(x,y) > Z_{\max} \\ \frac{Z(x,y) - Z_{\min}}{Z_{\max} - Z_{\min}} & Z_{\min} < Z(x,y) < Z_{\max} \\ 0 & Z(x,y) < Z_{\min} \end{cases} \quad (2)$$

where P is precipitation, Z is ground-surface elevation defined from the digital elevation model of the region, ξ is a dimensionless weight function, which is characterized by parameters Z_{\min} and Z_{\max} , and α is the fraction of precipitation that becomes recharge above Z_{\max} . Note that Z_{\min} defines the elevation below which no recharge occurs, and above elevation Z_{\max} the recharge is equal to αP . The total recharge flux Q over the model domain Ω is defined as

$$Q = \iint_{\Omega} R dx dy = \alpha \iint_{\Omega} \xi P dx dy = \alpha P' (Z_{\min}, Z_{\max}) \quad (3)$$

where P' is a function of Z_{\min} and Z_{\max} only. We assume $P(Z)$ is a simple linear model with fixed regression parameters, which we derive using annual precipitation data for the region (Spiegel and Baldwin 1963; Bowen 1992). Thus, there are four unknowns to be estimated (Q, α , Z_{\min} , and Z_{\max}) coupled through Equation 3. For example, to calculate Q we need to estimate α , Z_{\min} , and Z_{\max} . For our inverse models, we found it to be more computationally efficient to include Q, Z_{\min} , and Z_{\max} in the estimation process, and compute α as

$$\alpha = \frac{Q}{P' (Z_{\min}, Z_{\max})} \quad (4)$$

We simulate both steady-state (predevelopment) and transient (postdevelopment) conditions. Our transient simulations use municipal production data from wells operated by Los Alamos County and the City of Santa Fe and head measurements in nearby observation wells as calibration targets. We neglect the impact of undocumented withdrawals in the basin (both municipal and agricultural supply), which could approximately double the withdrawals accounted for in our model (Brian and Wilson 1997). Table 2 lists the water balance estimated by the basin model in

Table 2
Water Budget for the Basin Model, in kg/sec

Components	Steady-State Predevelopment (Year 1945)	Transient Postdevelopment (Year 1995)
Inflows		
Recharge	3845	3845
Flow from basins to the north	235	235
Release from aquifer storage	0	419
Total	4080	4499
Outflows		
Rio Grande	1112	1084
Tributaries	1389	1389
Flow to basins to the south and west	564	564
Pumping	0	448
Total	4080	4499

pre- and postdevelopment conditions. The documented withdrawals represent a relatively small proportion of the total fluxes through the aquifer (Table 2); and, even if we were able to account for undocumented withdrawals, the total would be still be relatively small. Because the wells we use for our transient head calibration dataset (predominantly in the western part of the basin) are far from areas of undocumented withdrawals (predominantly in the eastern part of the basin), neglecting this impact should have minimal only impact on the parameter estimates achieved through model calibration. Similarly, although aquifer recharge at rivers does occur in some locations, all reaches are still net discharge areas (shown as outflows in Table 2). Thus, while our model may be overestimating flux of water from the aquifer to river nodes, due to the assumption of perfect hydraulic connection, the simulated fluxes are still relatively small. Along all reaches, the predicted fluxes are much smaller than measured streamflow, supporting our assumption of constant head.

Hydrogeologic zones are defined by a three-dimensional geologic model for the basin (Carey et al. 1999). Zonation is defined primarily according to geologic features identified through field studies, geologic maps, interpretation of drillers logs, and geophysics (Vautaz et al. 1986; Baldridge et al. 1995; Smith et al. 1975; Kelley 1978; Manley 1979; Biehler et al. 1991; Ferguson et al. 1995; Dethier 1997). This process provides reasonably good control on contacts between Santa Fe Group rocks and other units in the basin; however, subdividing the Santa Fe Group rocks (the largest unit in the basin) could not be accomplished in this way. Therefore, we arbitrarily divided this unit into five broad geographic regions; later we test the validity of this subdivision using inverse modeling. The resulting model defines 23 geologic units, including two fault zones. A three-dimensional representation of the major units in the basin-scale model is shown in Figure 4.

Each node in the computational mesh is assigned to a unit according to its location relative to the three-dimensional hydrostratigraphic structure defined by the geologic model. Interpolation from the hydrostratigraphic model to the grid nodes is done by defining closed volumes for each

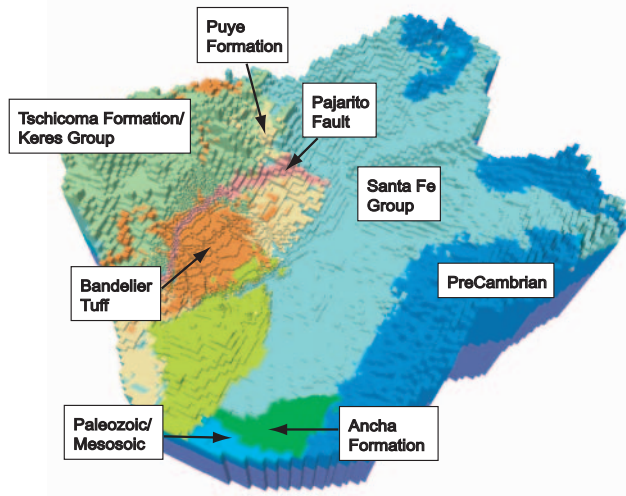


Figure 4. Three-dimensional representation of the major hydrostratigraphic units in the basin-scale model.

hydrostratigraphic unit. Each node of the mesh can be in one and only one of these volumes. The node properties are assigned based on which volume a node resides in. In this relatively simple approach, the location of contacts between hydrostratigraphic units can be resolved only to the degree of discretization in the finite element mesh. We use the parameter estimation process to determine the extent to which this zonation is justified, given the dataset available for model calibration. As described later, this process determined that some of the units should be combined. Although hydrogeologic zonation is defined for both site- and basin-scale models using the same three-dimensional geologic model, because of the increased vertical resolution in the site-scale model, we are able to represent hydrostratigraphic features with greater detail (Figures 3b and 3c).

Our model assumes confining conditions occur throughout the basin. Because of the strong anisotropy caused by beds within the Santa Fe Group, many pump tests throughout the region have indicated confined or leaky-confined conditions. Although some portions of the basin may, in fact, be unconfined, our approximation of confining conditions is a reasonable simplification given the substantial thickness of the aquifer (up to 3000 m) relative to drawdowns (0 to 100 m).

Model Coupling

We use the calibrated basin model to determine the total amount of water entering/exiting each of the four lateral site-scale model boundaries and along the top boundary (Q , precipitation recharge). Transient basin-model simulations demonstrate that, despite significant pumping within the site-scale model region, fluxes predicted by the basin model across the site-scale model boundaries do not change significantly with time. Rather, pumping is offset by a combination of release from storage and reduced discharge to the Rio Grande (Table 2). To allow for the possibility that recharge is distributed differently at the site scale than at the basin scale, we allow Z_{\min} to vary during site-scale model calibration.

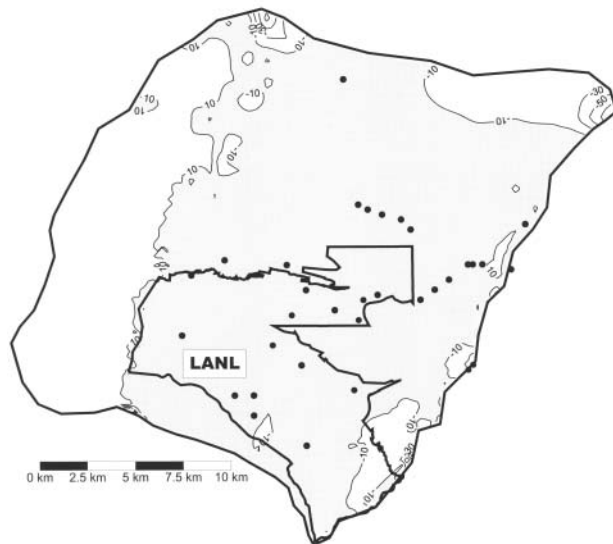


Figure 5. Differences in heads at the model top predicted by basin and site models, using identical parameter values. Gray area indicates agreement within 10 m. Solid dots represent location of calibration targets.

For the analyses presented in this paper, we use a relatively simple method of mapping fluxes at lateral site-scale model boundaries. Our method is spatially explicit; fluxes predicted by the basin model at each node corresponding to lateral site-scale model boundaries are mapped directly onto the corresponding site-scale model node. Site-scale model boundary nodes without corresponding basin nodes are modeled as no-flow. A more sophisticated flux mapping scheme, such as one that would distribute fluxes from each basin node to the multiple corresponding site-scale boundary nodes, might be necessary in situations where a high degree of accuracy is important very close to the model interface.

We first test our flux-mapping methodology using a site-scale model with exactly the same grid resolution as the basin-scale model. Using identical model parameters, these two models produce exactly the same head distributions. Mapping the same fluxes onto the high-resolution site-scale model, however, produced changes in these heads. Figure 5 shows the difference between basin- and site-scale model head predictions at the top of the model. These differences are primarily due to the enhanced detail in the site-scale representation of hydrostratigraphy. This scaling effect causes differences in the effective permeability of some units. The effect of differing representation of the Pajarito Fault zone is particularly evident, as a sharp increase in model error occurs west of the fault zone (Figure 4). In addition, our simplified flux mapping scheme causes relatively small and localized errors near model boundaries.

Parameter Estimation

A major component of our analysis is the estimation of parameters for both basin- and site-scale models. We applied the code PEST (Doherty 2000), which allows us to quantitatively estimate not only the model parameters that

Table 3
Parameter Estimates Derived from Inverse Models

Parameters	Basin Model		Site Model		
	Estimates	Confidence Intervals ^b	Estimates	Confidence Intervals ^b	
Recharge					
Z _{min} [m]	2195.	177.	2214.	362.	
Recharge volume [m ³]	3844.56	511.89	218.45	(fixed ^a)	
Permeabilities (log₁₀[m²])					
Deep Basement	−15.56	8.64	−15.56	305.89	
Paleozoic/Mesozoic (P/M)	−15.01	3.18	−15.05	41.00	
Shallow Sangres	−12.62	0.24	na		
Fractured preCambrian	−13.07	0.58	na		
Pajarito fault zone (Paj. Fault)	−15.34	0.83	−15.34	27.08	
Tschicoma formation (Tt)	−12.99	0.20	−13.02	5.81	
Cerros del Rio basalts (Tb)	−12.16	0.19	−11.89	0.62	
Puye Faglomerate/Totavi Lentil (Tpf/Tpt)	−14.20	1.35	−14.37	2.71	
Santa Fe group – Paleo river deposits	horizontal Ts _{fuv} (xy)	−13.24	0.27	−13.39	0.35
	vertical Ts _{fuv} (z)	−15.53	0.87	−15.64	1.57
Santa Fe group – West	horizontal Ts _f (west, xy)	−13.24	0.16	−13.06	0.25
	vertical Ts _f (west, z)	−15.04	0.43	−15.53	0.87
Santa Fe group – East, Pojoaque	−14.08	0.41	na		
Santa Fe group – Airport	−12.58	0.79	na		
Santa Fe group – North	−13.44	0.49	na		
Santa Fe group - Ojo Caliente sandstone	−13.26	0.18	na		
Santa Fe group - Penasco embayment	−12.36	0.28	na		
Ancha formation	−12.26	0.51	na		
Specific Storage log ₁₀ [m ^{−1}] (Sy)	−3.86	0.38	−3.64	0.48	
^a Derived from basin inverse model					
^b Confidence limits are defined as estimated value ± confidence intervals.					
“na” indicates the hydrostratigraphic unit exists in basin model but not in site model.					

provide the best model-data fit, but also the uncertainty of these parameter estimates and the corresponding contribution to uncertainty associated with any model prediction. The code uses the Levenberg-Marquardt (Levenberg 1944; Marquardt 1963) optimization algorithm. The objective function subject to minimization is defined as

$$\Phi = [\mathbf{c} - \mathbf{f}(\mathbf{b})]^T \mathbf{W} [\mathbf{c} - \mathbf{f}(\mathbf{b})] \quad (5)$$

where \mathbf{c} is a vector [$N \times 1$] of optimization targets, \mathbf{b} is a vector [$M \times 1$] of model parameters, \mathbf{W} is a diagonal weight matrix [$N \times M$], and \mathbf{f} is our nonlinear model. By minimizing Φ , the algorithm searches for the optimal parameter set \mathbf{b} that provides the best fit between simulated $\mathbf{f}(\mathbf{b})$ and measured \mathbf{c} quantities. The optimal parameter set \mathbf{b} will be also maximum likelihood if the residuals $\mathbf{c} - \mathbf{f}(\mathbf{b})$ are unbiased and normally distributed as well as if the model \mathbf{f} is linear. The vector of optimization targets includes (1) predevelopment (no pumping) steady-state heads and fluxes to the rivers along reaches, and (2) transient heads over a 50-year development period (Keating et al. 2000a). For the purposes of computational efficiency, we compare simulated to measured heads at time intervals varying from 5 to 20 years. The vector of estimated model parameters includes the recharge parameters (Q , Z_{\min} , Z_{\max}); permeability (k) of the various hydrostratigraphic units; and the globally uniform specific storage (S_s). The total recharge Q available to the site model is determined

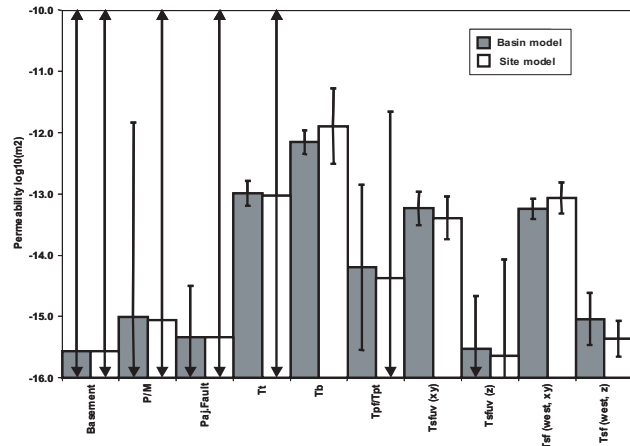


Figure 6. Parameter estimates for basin- and site-scale models; error bars represent the 95% linear confidence intervals of estimates (some of the error bars extend outside the figure limits; see Table 3).

by the basin model; during site model calibration, we allow only redistribution of Q over the model domain by varying Z_{\min} . The weight matrix \mathbf{W} defines the relative weight of each optimization target. The weights of steady-state and transient head targets vary from 0.3 to 3 m⁻¹ and depend on the subjective assessment of the measurement errors. The weights of flux targets are based on the standard variation of baseflow records. Common targets for both models have

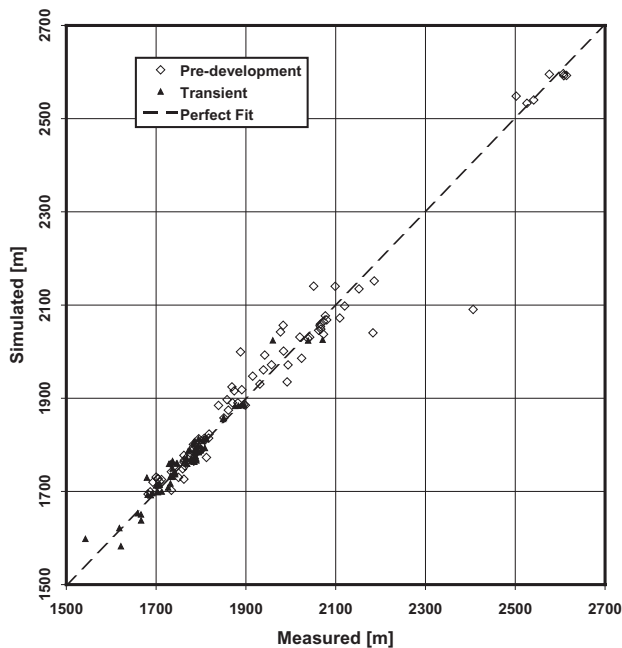


Figure 7. Comparison between measured and simulated heads in the basin-scale model.

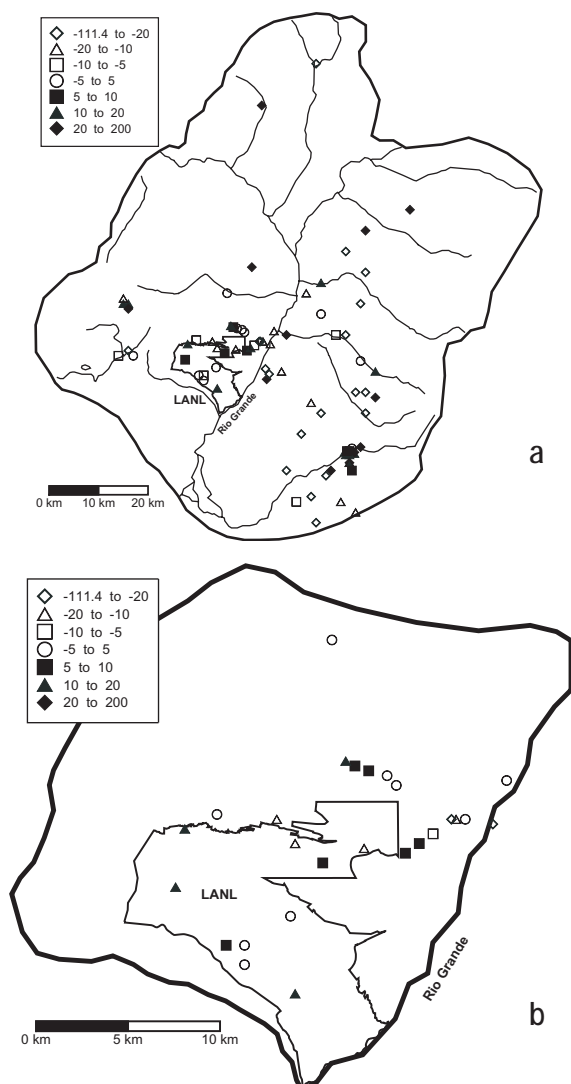


Figure 8. Spatial distribution of predevelopment calibration head targets and magnitude of residuals in the (a) basin-scale and (b) site-scale models.

equivalent weights. The calibration data are summarized in Table 1. The details of our procedure and results are described in Keating et al. (2000a).

The basin-scale inverse model analyzed 38 model parameters that include three recharge parameters, 35 permeabilities, and one specific storage. Our inverse analyses demonstrated that the data support the conceptual model that little or no recharge occurs at low elevations; in fact, Z_{\min} can be identified to within a few hundred meters. However, the data do not support the existence of a transitional zone between areas of no recharge ($\xi = 0$) and constant recharge fraction ($\xi = 1$), as defined in Equation 2. Therefore, we set Z_{\max} equal to Z_{\min} , and the number of recharge parameters is decreased to two. The 35 permeabilities are defining the properties of 23 hydrostratigraphic units and two fault zones. All the units and fault zones are assumed to be uniform; most are assumed to be isotropic. For some, we have attempted to distinguish between horizontal and vertical permeability components, but the available data allow this only for two of the Santa Fe Group sub-units (Paleo river deposits and West). Analyses of parameter sensitivities and covariance eigenvectors (Keating et al. 2000a) suggested that the available data could not support the degree of detail present in the hydrostratigraphic model; nine of the defined zones (eight units and one fault zone) should be combined with other zones. After simplifying the model structure in this way, the number of permeabilities estimated by the inverse model is 18 (14 isotropic units, including the Pajarito Fault Zone, and two units with horizontal and vertical components), as shown in Table 3. As shown in the table, most of the parameters are \log_{10} transformed in the estimation process.

The parameter estimates and their respective 95% linear confidence intervals (confidence limits are defined as estimated value \pm confidence intervals) are listed in Table 3 and illustrated in Figure 6. Our parameter estimation errors ranged widely. For example, recharge parameters, Z_{\min} and Q , are estimated with the high certainty; the corresponding value of α is 8.4%, which is close to the values reported in the literature (Anderholm 1994; Wasiolek 1995). The permeabilities of the very deep hydrostratigraphic units in the basin (below any wells) are poorly constrained (Basement, P/M). Details about the analysis of inverse model results can be found in Keating et al. (2000a). By means of eigenvector analysis of estimation errors, we demonstrated that the uncertainty for some of the units is predominantly due to the cross-correlations of estimation errors rather than low parameter sensitivities to the observations. Comparisons between inverse models with and without the transient head data in reducing estimation uncertainty for several key hydrostratigraphic units. Analyses of partial derivatives of observations with respect to parameter sensitivity (Jacobian matrix) demonstrated the importance of the flux targets in constraining most of the estimated parameters.

The basin-model matches of the head and flux targets are presented in Figures 7, 8, and 9, respectively. The figures demonstrate that our model represent the observed data well. There are two outliers in Figure 7 that are associated with wells far from regions of interest (northern por-

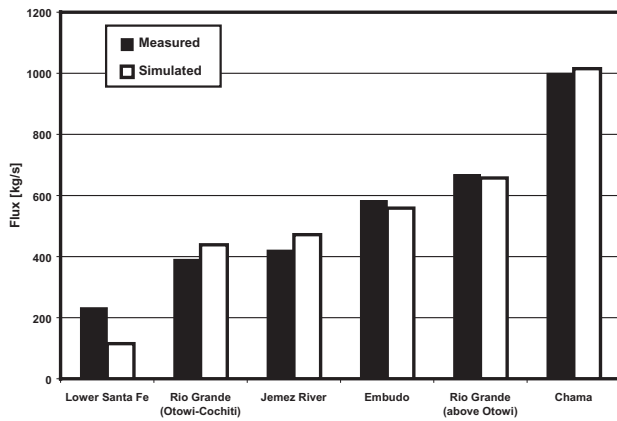


Figure 9. Comparison between measured and simulated fluxes in the basin-scale model.

Table 4
Descriptive Statistics and Normality Test Results
for the Dimensionless Weighted Residuals

	Basin Model	Site Model
Statistics		
Minimum	-117	-57
Maximum	92	115
Mean	1.75	0.07
Standard deviation	38.1	38.2
Skewness	0.05	0.94
Kurtosis	0.31	0.63
Non-parametric Kolmogorov-Smirnov normality test		
Maximal difference	0.48	0.11
Minimal difference	-0.33	-0.08
Z value	0.621	1.029
p value	84% (> 5%)	24% (> 5%)

tion of the basin) and could be due to measurement errors (perched versus regional aquifer measurements). Figure 8 presents the spatial distribution of residuals for the predevelopment simulations. The weighted residuals between simulated and observed measurements are unbiased (centered around zero) and their distribution is close to normal. The descriptive statistics and normality test results are listed in Table 4. The test for normality of the residual distributions is performed using the Kolmogorov-Smirnov nonparametric test (Hollander and Wolfe 1973). The Z value is calculated from the largest absolute difference between the observed and the theoretical (in this case normal) distribution. Because the p-value (asymptotic significance level) for the test is greater than 5%, the hypothesis that the residuals are normally distributed cannot be rejected.

Most of the site- and basin-model permeability estimates are similar. However, there are substantial discrepancies for the vertical permeability of Santa Fe Group (west) and permeability of Cerros del Rio basalts; the site-model estimate for the basalts is outside the confidence limits estimated by the basin model. Many factors may be contributing to the disparity in the model estimates: different grid resolution (Figure 3), which affects the delineation of hydrostratigraphic units and spatial representation of observation targets, and

differences in the calibration set. All the calibration targets used in the site model are also defined in the basin model; the sum of squared residuals for the common targets in both models are similar (Table 1). Overall, the site-model estimates are associated with higher uncertainty compared to the basin model. Additional data would be needed to decrease the estimation uncertainty of model parameters.

Uncertainties in Basin-Scale Flux Predictions

As described earlier, we use the basin model to estimate boundary fluxes for the site-scale model. These estimates, like any other model predictions, are undoubtedly uncertain. Possible sources of uncertainty include conceptual model errors, parameterization errors, discretization (grid-resolution) errors, measurement errors, and uncertainty in model parameters (Carrera 1984). Owing to low model sensitivity and correlations among parameter estimates, there may be multiple parameters sets that produce equally well-calibrated results (as measured by our objective function), but provide quite different predictions.

One way to address this problem is through sensitivity analysis. However, sensitivity analysis of model parameters to the predictions provides us with information only about the degree of dependence between the parameters and the predictions in the close vicinity of the optimal estimates. Therefore, sensitivity analysis has limited applicability due to nonlinearity of the forward problem and the cross-correlations between estimates. A better approach is to estimate the nonlinear confidence limits of our predictions (Vecchia and Cooley 1987). We have performed this using the predictive analysis tool in PEST (Doherty 2000), which estimates uncertainty in the model predictions by constrained nonlinear optimization of the inverse model. The predictive algorithm in PEST allows estimation of a set of model parameters that not only reproduce observations within a specified tolerance but also either maximize or minimize the analyzed prediction. The search in parameter space is performed within a predefined limit of the objective function. The analysis allows an efficient, though computationally intensive, way to determine the impact of parameter uncertainty on the model predictions. The prediction p is defined as

$$p = f'(\mathbf{b}) \quad (6)$$

where f' is our model under predictive conditions. We search for \mathbf{b} that either maximizes or minimizes p subject to the constraint

$$[\mathbf{c} - \mathbf{f}(\mathbf{b})]^T \mathbf{W} [\mathbf{c} - \mathbf{f}(\mathbf{b})] \leq \delta \Phi_{\min} \quad (7)$$

where Φ_{\min} is defined for the maximum likelihood estimates \mathbf{b}_{ML} using Equation 5, and δ is defined as (Bard 1974)

$$\delta = \frac{\mathbf{B}}{\mathbf{N} - \mathbf{M}} \mathbf{F}_a(\mathbf{N}, \mathbf{N} - \mathbf{M}) + 1 \quad (8)$$

where F is the F distribution and a is the confidence level. Due to nonlinearity of our model, the optimal estimates \mathbf{b}_{opt} obtained in the optimization process are not strictly maxi-

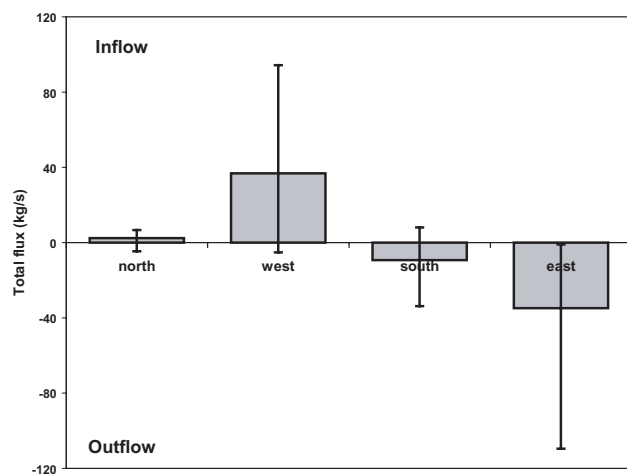


Figure 10. Fluxes across lateral site-model boundaries predicted by calibrated basin model; error bars represent the 95% nonlinear confidence intervals of estimates.

mum likelihood estimates. However, we take \mathbf{b}_{opt} to be an approximation of \mathbf{b}_{ML} , as typically done in the literature (Carrera 1984). The nonlinear constrained optimization is solved as an iterative Lagrangian problem as proposed by Vecchia and Cooley (1987). The obtained range in predictions represent the nonlinear confidence limits. Previous applications of this approach can be found in Keating et al. (2000b) and Vesselinov et al. (2001, 2002).

We apply this approach to estimate the nonlinear confidence limits of predicted predevelopment flux across each of lateral site-model boundaries using the basin inverse model. Figure 10 shows the predictions and their uncertainty. Figure 10 illustrates the relatively high certainty for the predicted north and south fluxes and the relatively low certainty for the predicted flux across the western boundary. The high uncertainty in the western flux is partially due to the overall direction of the ground water flow, which within the site-scale domain is from west to east. More important, the western flux is almost entirely controlled by the permeability of the Pajarito Fault (Figure 4), which is associated with relatively high uncertainty (Table 3). In our analysis, we have included the east site model boundary, which is located beneath the constant head boundary. It is commonly assumed under similar ground water conditions that there should be a ground water divide beneath the river so it can be represented in a model as a no-flow boundary (Freeze and Cherry 1979). However, our analysis suggests that there is flow beneath the river and its uncertainty is relatively high (Figure 4) because of the heterogeneity of medium properties and the spatial distribution of precipitation recharge. More detailed analysis of this phenomenon and its impact on the distribution of ground water resources can be found in Vesselinov and Keating (2002).

For the purpose of comparison, we have also computed the 95% linear confidence intervals (Seber and Wild 1989, p. 193) of predicted flux across each of lateral site-model boundaries. We found that the linear confidence intervals not only significantly overestimated the uncer-

tainty (two order of magnitudes higher than the nonlinear intervals, defining a wide range of unrealistic fluxes) but also were uncorrelated with the nonlinear counterparts (linear intervals predict the highest uncertainty to be associated with the southern flux, which has low uncertainty according to the nonlinear analysis).

Given the uncertainty in predicted lateral fluxes evident in Figure 10, we can test the sensitivity of site-scale model predictions to this range of possible boundary fluxes. Here we present one sensitivity analysis, using advective transport simulations at the site scale. We use particle tracking to determine the advective travel time from a site near the western boundary of LANL to the discharge point (Rio Grande). Elsewhere, we have demonstrated (Keating et al. 2000) that these travel times are very sensitive to uncertainty in model parameters (recharge, permeability, and porosity). Here, we investigate sensitivity to fluxes at model boundaries. To accomplish this, we simulate transport using six flow fields, each with boundary conditions specified according to the results shown in Figure 10. It must be stressed that each predictive analysis result provides flux estimates not only for the boundary of interest but also the other three. We compared travel times predicted by the calibrated model to the times predicted using each of the six flow fields representing “extreme” boundary fluxes and found that results differed by 20% or less. This variation is much lower than that due to other uncertain model parameters (Keating et al. 2000). This result allows us to concentrate on other sources of model uncertainty in our future analyses. It is important to note, however, that this result is specific to this particular model prediction and cannot be generalized to other model applications.

Conclusions

We have presented a high-resolution site-scale model nested within a basin-scale model, coupled via fixed-flux conditions at all site-model boundaries. Hydrostratigraphy for both models is derived from a single three-dimensional geologic model. However, because of differences in grid resolution the hydrostratigraphy is represented with greater detail in the site-scale model. Because of this, if the two models are parameterized identically there will be differences in simulated heads.

The basin-scale model provided not only estimates of the coupling fluxes along the site-scale model boundaries, but also provided important information about their predictive uncertainty. We use inverse modeling to estimate the parameters and their uncertainty for the two models. The results show that parameter estimates are similar overall but there are some specific differences. Parameter uncertainty is quite different at the two scales. This is due to several factors, including differences in the resolution of the model grids (scale of parameter estimation and differences in spatial representation of calibration targets) and differences in the number and types of calibration targets. Therefore, we caution against application of permeability estimates obtained by basin-scale modeling for predictions using a nested site-scale model, and vice versa.

We have applied a robust (although computationally intensive) method to evaluate the uncertainty in our basin-scale model predictions of fluxes to the site-scale model. This method is preferable to conventional sensitivity analysis because it explicitly considers uncertainty in all parameters and results are limited to combinations of model parameters that fall within specified model calibration criteria. Through this exercise, we have determined that fluxes to some lateral site-model boundaries are quite well constrained by basin-model predictions; however, other lateral boundaries are far more uncertain. Site-scale model predictions of advective travel times are relatively insensitive to the uncertainty in these boundary fluxes; therefore, other sources of uncertainty should be given higher priority for future work.

Future work on the coupling of basin- and local-scale inverse models will include more rigorous analysis of propagation of uncertainty between the models, and evaluation of not only prediction but also estimation uncertainty in the local-scale inverse model due to uncertainty in the coupling predicted by the basin-scale inverse model.

Acknowledgments

This work has been supported by the Department of Energy and the Los Alamos National Laboratory Hydrogeologic Characterization Program. We are grateful for contributions by Greg Cole, Bill Carey, and Carl Gable in development of the hydrostratigraphic framework model and computational grids.

References

- Anderholm, S.K. 1994. Ground-water recharge near Santa Fe, north-central New Mexico. U.S. Geological Survey Water Resources Investigations Report 94-4078.
- Anderson, M., and W.W. Woessner. 1992. *Applied Groundwater Modeling*. San Diego: Academic Press.
- Baldrige, W.S., J.F. Ferguson, L.W. Braile, B. Wang, K. Eckhardt, D. Evans, C. Schultz, B. Gilpin, G.R. Jiracek, and S. Biehler. 1995. The western margin of the Rio Grande Rift in northern New Mexico: An aborted boundary? *GSA Bulletin* 105, 1538–1551.
- Bard, M. 1974. *Nonlinear Parameter Estimation*. New York: Academic Press.
- Biehler, S.J., J. Ferguson, W.S. Baldrige, G.R. Jiracek, J.L. Aldern, M. Martinez, R. Fernandez, J. Romo, B. Gilpin, and L.W. Braille. 1991. A geophysical model of the Espanola Basin, Rio Grande Rift, New Mexico. *Geophysics* 56, no. 3: 340–353.
- Bowen, B.M. 1992. Los Alamos climatology summary including latest normals from 1961–1990. Los Alamos National Laboratory Report LA-12232-MS. <http://lib-www.lanl.gov/lapubs/00194103.pdf>.
- Brian, C., and P.E. Wilson. 1997. Water use by categories in New Mexico counties and river basins, and irrigated acreage in 1995. New Mexico State Engineer Office, Technical Report, Santa Fe, New Mexico.
- Carey, B., G. Cole, C. Lewis, F. Tsai, R. Warren, and G. Wolde-Gabriel. 1999. Revised site-wide geologic model for Los Alamos National Laboratory. Los Alamos National Laboratory Report LA-UR-00-2056. <http://lib-www.lanl.gov/lapubs/00393599.pdf>.
- Carrera, J. 1984. Estimation of aquifer parameters under transient and steady state conditions. Ph.D. thesis, University of Arizona, Tucson, Arizona.
- Coon, L.M., and T.E. Kelly. 1984. Regional hydrogeology and the effect of structural control and the flow of ground water in the Rio Grande trough, northern New Mexico. New Mexico Geological Society Guidebook, 35th Field Conference, Rio Grande Rift, Northern New Mexico, 241–244.
- Cordell, L. 1979. Gravimetric expression of graben faulting in Santa Fe County and the Espanola Basin, New Mexico. New Mexico Geological Society Guidebook, 30th Field Conference, Santa Fe County, 59–64.
- Daniel B. Stephens & Associates Inc. 1994. Santa Fe County water resource inventory. Santa Fe, New Mexico: Daniel B. Stephens and Associates Inc.
- Dethier, D.P. 1997. Geology of White Rock quadrangle, Los Alamos and Santa Fe counties, New Mexico. New Mexico Bureau of Mines & Mineral Resources Geologic Map.
- Doherty, J. 2000. PEST: Model Independent Parameter Estimation. Brisbane, Australia: Watermark Computing.
- Ferguson, J.F., W.S. Baldrige, L.W. Braile, S. Biehler, B. Gilpin, and G.R. Jiracek. 1995. Structure of the Espanola Basin, Rio Grande Rift, New Mexico, from SAGE seismic and gravity data. New Mexico Geological Society Guidebook, 46th Field Conference, Geology of the Santa Fe Region, 105–109.
- Frenzel, P.F. 1995. Geohydrology and simulation of ground-water flow near Los Alamos, north central New Mexico. U.S. Geological Survey Water Resources Investigations Report 95-4091.
- Freeze, R.A., and J.A. Cherry. 1979. *Groundwater*. New Jersey: Prentice Hall.
- Giudici, M., G. Parravicini, G. Ponzini, E. Romano, and D. Villa. 2001. Nested models to simulate groundwater flow at different scales. *Geophysical Research Abstracts* 3, 2086.
- Hearne, G.A. 1985. Mathematical model of the Tesuque aquifer system underlying Pojoaque River Basin and vicinity, New Mexico. U.S. Geological Survey Water-Supply Paper 2205.
- Hollander, M., and D.A. Wolfe. 1973. *Nonparametric Statistical Methods*. New York: John Wiley & Sons.
- Hunt, R., J. Steuer, M. Mansor, and T. Bullen. 2001. Delineating a recharge area for a spring using numerical modeling, Monte Carlo techniques, and geochemical investigation. *Ground Water* 39, no. 5: 702–712.
- Keating, E.H., and J.M. Bahr. 1998. Using reactive solutes to constrain groundwater flow models at a site in northern Wisconsin. *Water Resources Research* 34, no. 12: 3561–3571.
- Keating, E.H., E. Kwicklis, V. Vesselinov, A. Idar, Z. Lu, G. Zyzolowski, and M. Witkowski. 2000a. A regional flow and transport model for groundwater at Los Alamos National Laboratory. Los Alamos National Laboratory Report LA-UR-01-2199, <http://lib-www.lanl.gov/lapubs/00818241.pdf>.
- Keating, E.H., J. Doherty, and V. Vesselinov. 2000b. Approaches to quantifying uncertainty in flow directions in the regional aquifer beneath the Pajarito Plateau, northern New Mexico. *Supplement to EOS Transactions* 81, no. 48: F511.
- Keating, E.H., E. Kwicklis, M. Witkowski, and T. Ballantine. 1999. A regional flow model for the regional aquifer beneath the Pajarito Plateau. Los Alamos National Laboratory Report LA-UR-00-1029.
- Keating, E.H., and V.V. Vesselinov. 2001. A comparison of two approaches to modeling capture zones at the site-scale: Adaptive mesh refinement within a basin-scale model and site-scale/basin-scale model coupling. *Eos. Trans. AGU* 82, no. 47, Abstract H22D-0383.
- Kelley, V.C. 1978. *Geology of the Espanola Basin*. New Mexico Bureau of Mines and Mineral Resources Map.
- Kernodle, J.M.D.P.M., and C.R. Thorn. 1995. Simulation of ground-water flow in the Albuquerque Basin, central New Mexico, 1901–1994, with projections to 2020. USGS Water-Resources Investigation Report 94-4251.
- Los Alamos National Laboratory. 1998. *Hydrogeologic Workplan*. Environment, Safety, and Health Division, LANL, Los Alamos, New Mexico, LAUR 01-6511.

- Leake, S., P. Lawson, M. Lilly, and D. Claar. 1998. Assignment of boundary conditions in embedded ground water flow models. *Ground Water* 36, no. 4: 621–625.
- Levenberg, K.A. 1944. A method for the solution of certain nonlinear problems in least squares. *Quarterly of Applied Mathematics* 2, 164–168.
- Manley, K. 1979. Stratigraphy and structure of the Espanola Basin, Rio Grande Rift, New Mexico. In *Rio Grande Rift: Tectonics and Magmatism*, ed. R.E. Riecker, 71–86. American Geophysical Union Special Publication.
- Marquardt, D.W. 1963. An algorithm for least-squares estimation of nonlinear parameters. *Journal of the Society of Industrial and Applied Mathematics* 11, no. 3: 431–441.
- McAda, D.P., and M. Wasiolek. 1988. Simulation of the regional geohydrology of the Tesuque aquifer system near Santa Fe, New Mexico. U.S. Geological Survey Water Resources Investigations Report 87-4056.
- Meier, P.M., J. Carrera, and X. Sanchez-Vila. 1999. A numerical study on the relationship between transmissivity and specific capacity in heterogeneous aquifers. *Ground Water* 37, no. 4: 611–617.
- Purtymun, W.D. 1984. Hydrologic characteristics of the main aquifer in the Los Alamos area: Development of ground water supplies. Los Alamos National Laboratory Report LA-995.
- Purtymun, W.D., and S. Johansen. 1974. General geohydrology of the Pajarito Plateau. New Mexico Geologic Society Guidebook, 25th Field Conference.
- Purtymun, W.D., A.K. Stoker, and S.G. McLin. 1995. Water supply at Los Alamos during 1993. Los Alamos National Laboratory Report LA-12951-PR.
- Seber, G.A.F., and C.J. Wild. 1989. *Nonlinear Regression*. New York: John Wiley & Sons.
- Smith, R.L., R.A. Bailey, and C.S. Ross. 1975. Geologic map of the Jemez Mountains, New Mexico. U. S. Geological Survey Miscellaneous Investigations Series Map.
- Spiegel, Z., and B. Baldwin. 1963. Geology and water resources of the Santa Fe area. U.S. Geological Survey Water-Supply Paper 1525.
- Tiedeman, C.R., J.M. Kernodle, and D.P. McAda. 1998. Application of nonlinear-regression methods to a ground-water flow model of the Albuquerque Basin, New Mexico. U.S. Geological Survey Water-Resources Investigations Report 98-4172.90.
- Trease, H., D. George, C.W. Gable, J. Fowler, A. Kuprat, and A. Khamyaseh. 1996. The X3D grid generation system. In *Numerical Grid Generation System in Computational Fluid Dynamics and Related Fields*, ed. B.K. Soni, J.F. Thompson, H. Hausser, and P.R. Eiseman, 1129. Starkville, Mississippi: Mississippi State University.
- U.S. Geological Survey. 1997. WATSTORE database.
- U.S. Geological Survey. 2001. Surface-Water Data for USA. <http://water.usgs.gov/nwis/sw>.
- Vautaz, F.D., F. Goff, C. Fouillac, and J.Y. Calvez. 1986. Isotope geochemistry of thermal and nonthermal waters in the Valles Caldera, Jemez Mountains, northern New Mexico. *Journal of Geophysics Research* 91, 1835–1853.
- Vecchia, A.V., and R.L. Cooley. 1987. Simultaneous confidence and prediction intervals for nonlinear regression models with application to a groundwater flow model. *Water Resources Research* 23, no. 7: 1237–1250.
- Vesselinov, V.V., E.H. Keating, and J. Doherty. 2001. Analysis of uncertainty in model predictions of flow and transport in the Espanola Basin regional aquifer, northern New Mexico. *Eos. Trans. AGU* 82, no. 47, Abstract H12D-0329.
- Vesselinov, V.V., and S. Neuman. 2001. Numerical inverse interpretation of single-hole pneumatic tests in unsaturated fractured tuff. *Ground Water* 39, no. 5: 685–695.
- Vesselinov, V.V., and E.H. Keating. 2002. Analysis of capture zones of the Buckman Wellfield and a proposed new horizontal collector well north of the Otowi Bridge, Los Alamos National Laboratory Report LA-UR-02-2750.
- Vesselinov, V.V., E.H. Keating, and G.A. Zyvoloski. 2002. Analysis of model sensitivity and predictive uncertainty of capture zones in the Espanola Basin regional aquifer, northern New Mexico. *International Conference ModelCARE 2002 Calibration and Reliability in Groundwater Modeling: A Few Steps Closer to Reality*, Prague, Czech Republic, 17–20.
- Walker, D., and B. Gylling. 1998. Site-scale groundwater flow modelling of Aberg. Swedish Nuclear Fuel and Waste Management Company Technical Report, TR-98-23.167.
- Ward, D.S., D.R. Buss, J.W. Mercer, and S.S. Hughes. 1987. Evaluation of a groundwater corrective action at the Chem-Dyne hazardous waste site using a telescopic mesh refinement modeling approach. *Water Resources Research* 23, no. 4: 603–617.
- Wasiolek, M. 1995. Subsurface recharge to the Tesuque aquifer system from selected drainage basins along the western side of the Sangre de Cristo Mountains near Santa Fe, New Mexico. U.S. Geological Survey Water-Resources Investigations Report 94-4072.
- Zyvoloski, G., E. Kwicklis, A. Eddebbarh, B. Arnold, C. Faunt, and B.A. Robinson. 2002. The site-scale saturated-zone flow model for Yucca Mountain: Calibration of different conceptual models and their impact on transport. *Journal of Contaminant Hydrology*, in press.
- Zyvoloski, G.A., B.A. Robinson, Z.V. Dash, and L.L. Trease. 1997. Summary of the models and methods for the FEHM application: A finite-element heat- and mass-transfer code. Los Alamos National Laboratory Report LA-13306-MS.